Proceedings of the XXXVI Zakopane School of Physics, Zakopane 2001

Application of ^{172}Yb in Perturbed Angular Correlation Measurements

M. Rams* and K. Królas

Institute of Physics, Jagiellonian University
Reymonta 4, 30-059 Kraków, Poland

The radioactive decay of ^{172}Lu $\rightarrow$ ^{172}Yb appears to be suitable for time-differential perturbed angular correlation measurements of quadrupole interaction. The technique was applied to study various phenomena in three compounds: Yb_3S_4, $YbPO_4$, $Yb_2Co_3Ga_9$. We were able to distinguish between Yb^{2+} and Yb^{3+} ions occupying different positions in the crystal lattice of Yb_3S_4. Crystal electric field parameters reproduced the temperature dependence of the quadrupole interaction of Yb in $YbPO_4$. Finally, the influence of hybridization on the $4f$ quadrupole moment in $Yb_2Co_3Ga_9$ is evidenced.

PACS numbers: 76.80.+y, 75.10.Dg, 75.30.Mb

1. Introduction

Nuclear spectroscopic techniques such as nuclear magnetic and quadrupole resonances and the Mössbauer spectroscopy have proved to be useful in studying structural and electronic properties of anomalous rare-earth materials in a microscopic way. An application of these techniques is limited to compounds of certain elements since each method requires an isotope with specific properties of the nuclear ground or excited state. At present many experiments are performed using the Mössbauer effect and nuclear quadrupole resonance (NQR) with several lanthanide isotopes. On the contrary, only few perturbed angular correlation (PAC) experiments with rare-earth elements have been carried out up to now. Over thirty years ago, it was shown [1] that ^{172}Yb fulfills requirements of the PAC technique. However, until several years ago this isotope was not applied to studies of solid state physics problems. This article characterizes ^{172}Yb as a PAC probe and presents several recent examples which illustrate that the PAC method can successfully answer various questions about properties of ytterbium compounds.

*corresponding author; e-mail: uframs@if.uj.edu.pl

2. The basis of PAC

In the perturbed angular correlation technique a hyperfine interaction is observed through quantum beats in the angular distribution of γ rays emitted by a radioactive probe nucleus. A cascade of two consecutive γ rays is observed by detectors, which are arranged under fixed angles. An event is counted when a pair of detectors registers both γ quanta. The counts are collected with respect to the time which elapsed from the first to the second emission, that is the time when the nucleus is in the intermediate state of the cascade and evolves in an external hyperfine field. The number of coincidences decreases with the delay time in the following way:

$$N(\theta,t) = N_0 \exp(-t/\tau)[1 + A_{22}G_{22}(t)P_2(\cos\theta)], \tag{1}$$

where θ is the angle between detectors, τ is the lifetime of the intermediate level in the cascade, P_2 is the second Legendre polynomial, A_{22} is the anisotropy of the cascade. The perturbation factor $G_{22}(t)$ contains all relevant information on type and strength of the hyperfine interaction. To extract $G_{22}(t)$ the detectors are arranged under angles of 90° and 180° and the following experimental ratio is calculated:

$$R(t) = 2[N(180°,t) - N(90°,t)]/[N(180°,t) + 2N(90°,t)] = A_{22}G_{22}(t). \tag{2}$$

For a static, electric quadrupole interaction $G_{22}(t)$ is an oscillating function, the quadrupole coupling constant $\nu_Q = eQV_{zz}/h$, where Q is the quadrupole moment of the intermediate nuclear state, and V_{zz} is the main component of the electric field gradient (EFG) acting upon the nucleus. The shape of $G_{22}(t)$ depends on the spin of the nuclear level and asymmetry parameter $\eta = (V_{xx} - V_{yy})/V_{zz}$. Perturbation factors for different asymmetry parameters, for spins $I = 2$ and $I = 3$ are shown in Fig. 1. Complete overviews of the PAC theory and technique were presented in Refs. [2] and [3].

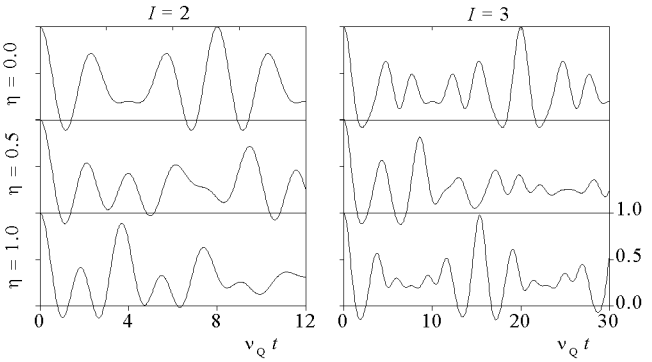

Fig. 1. G_{22} factors for electric quadrupole interaction with different asymmetry parameter η for spins $I = 2$ and $I = 3$.

3. ^{172}Yb as a PAC probe

The choice of ^{172}Yb was imposed by requirements, which have to be met by a probe in time-differential perturbed angular correlation measurements. To be a good PAC probe a nucleus needs an excited state with half-life of the order of nanoseconds, with a spin greater than 1/2 and with a nonzero quadrupole moment. A cascade of gamma rays going through this state should have significant intensity and anisotropy. Finally, an easy production of the isotope is required. Among all isotopes of all rare-earth elements, the ^{172}Lu $\rightarrow$ ^{172}Yb decay is the only one, which meets the above requirements in the way making routine measurements possible. Two different γ–γ cascades can be used: 91–1094 keV and 1094–79 keV. In Table I basic data about both cascades are gathered and a comparison with the most commonly used ^{111}In $\rightarrow$ ^{111}Cd decay in PAC studies is presented.

TABLE I

Comparison of ^{111}In $\rightarrow$ ^{111}Cd and ^{172}Lu $\rightarrow$ ^{172}Yb PAC probes.

	^{172}Lu $\rightarrow$ ^{172}Yb		^{111}In $\rightarrow$ ^{111}Cd
source $T_{1/2}$	6.7 d		2.8 d
production	^{172}Yb(d,2n)^{172}Lu		^{109}Ag(α,2n)^{111}In
number of γ lines in decay	101		2
cascade	91–1094 keV	1094–79 keV	171–245 keV
intensities of γ lines J	4.5–63%	63–10%	90-94%
intermediate level $T_{1/2}$	8.3 ns	1.65 ns	84.5 ns
spin I	3	2	5/2
quadrupole moment Q	–3.0(1) b	–2.21(6) b	0.77(12) b
magnetic moment gI	0.65(4)	0.69(16)	0.766(2)
anisotropy A_{22}	+0.28	–0.38	–0.18
efficiency Ω	660	400	130000

The lutetium activity can be obtained by deuteron or proton irradiation of a sample, which contains ytterbium. A convenient half-life of ^{172}Lu allows carrying out the PAC measurements up to several weaks after irradiation. The efficiency $\Omega = A_{22}J_1J_2T_{1/2}$ gives information about the quality of a cascade. The energy spectrum of natural Yb irradiated with 14 MeV deuterons (see Fig. 2) shows a great number of γ lines. The lines 79 and 91 keV are clearly visible in the spectrum taken with a semiconductor detector but they are totally covered by the background in the spectrum taken with a scintillator detector that has to be used in the PAC apparatus. It increases significantly the background of delayed coincidences and results in a decrease in the effective anisotropy.

The big difference between energies of two γ rays in both cascades forces to use different detectors. In our setup two BaF_2 3 mm thick crystals were used to

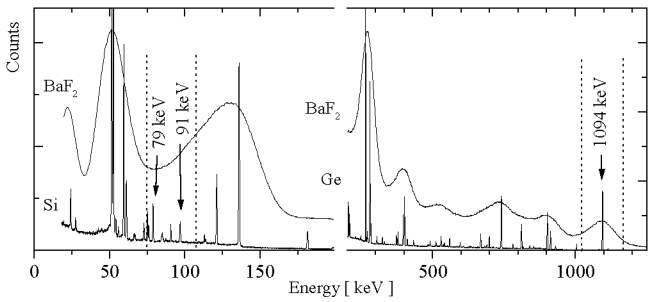

Fig. 2. Energy spectrum of Yb_4As_3, 7 days after deuteron irradiation observed with scintillation and semiconductor detectors. Dashed lines show chosen energy windows.

detect the 79 and 91 keV lines, while two $50\phi50$ mm thick BaF_2 crystals shielded with 1 mm Pb, Cd, and Cu foils were used to detect the 1094 keV line. As a consequence, only four pairs of counters collected only four PAC spectra, while twelve spectra would be collected in a setup consisting of four identical detectors.

On the other hand, similar energies of 79 and 91 keV lines make it possible to collect spectra for both cascades simultaneously. One of four PAC time spectra is shown in Fig. 3 together with extracted perturbation factor $R(t)$ below. Decays of both excited levels are seen on the left and right sides of $t = 0$. The shapes of the perturbation factor differ from each other because of different nuclear spins, but the obtained hyperfine fields are the same. The comparison of EFGs obtained simultaneously from two different cascades is a very good test whether all spectra were correctly fitted.

Ytterbium compounds can be successfully investigated with the Mössbauer effect using ^{170}Yb [4]. In Table II a short comparison of advantages and limitations of both techniques is presented. These two methods complement one another. At low temperatures, where V_{zz} can reach big values (up to about 600 V/Å^2), the Mössbauer spectroscopy (MS) can be used. At high temperatures, where V_{zz} is usually small, only PAC is usable.

4. Origin of EFG in rare-earth compounds

In rare-earth compounds the EFG tensor V_{ij} originates from two significant sources. The first contribution arises, at the nuclear site of a rare-earth ion, from charges of the surrounding ions in the lattice. The second one is provided by the own electrons of the probe ion, i.e. by the non-spherical $4f$ shell

$$V_{ij}(T) = V_{ij}^{\mathrm{lat}} + V_{ij}^{4f}(T). \tag{3}$$

The lattice contribution is practically temperature independent, neglecting a small decrease with temperature due to a lattice expansion and thermal vibrations. By contrast, the $4f$ electron contribution usually strongly depends on temperature. It is determined by the electronic state of the ion. The paramagnetic Yb^{3+} ion

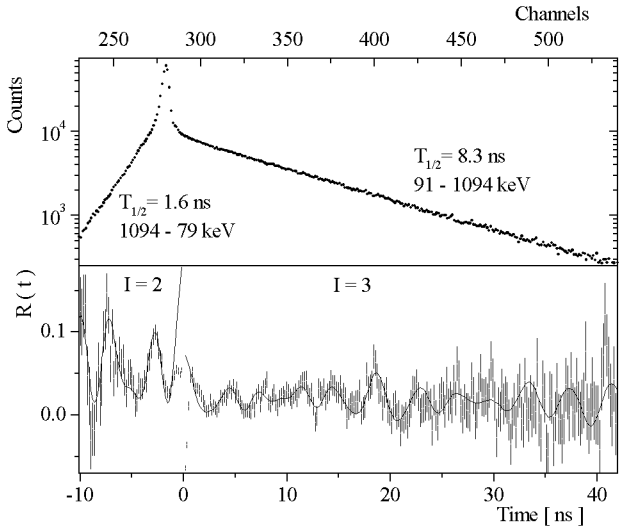

Fig. 3. PAC time spectrum and extracted perturbation factors taken with ^{172}Yb probe in Yb_2O_3 at $T = 295$ K.

TABLE II

Advantages (+) and limitations (–) of the ^{170}Yb Mössbauer spectroscopy and ^{172}Yb PAC.

PAC with ^{172}Yb	MS with ^{170}Yb
+ sensitivity independent of temperature	– temperatures only up to 80 K
+ good sensitivity to EFG (5 V/Å^2)	– weak sensitivity to EFG (20 V/Å^2)
– V_{zz} limited up to about 300 V/Å^2	+ V_{zz} without limits
– sign of V_{zz} cannot be determined	+ sign of V_{zz} can be measured

has an incomplete $4f$ shell with one hole in it. In solids, the crystal electric field (CEF) splits the $^2F_{7/2}$ ground state into 4 Kramers doublets with a typical overall splitting of the order of a few hundred kelvins. Each occupied $4f$ doublet gives its own, different contribution to the EFG at the nucleus. The average EFG is expected to vary strongly with temperature according to the varying Boltzmann occupation of the Kramers doublets. At low temperatures, when the ion is in its lowest energy state, the $4f$ contribution is usually dominant. At the limit of high temperatures, when all Kramers states are equally populated, the $4f$ contribution vanishes and only the lattice contribution is present.

A diamagnetic Yb^{2+} ion has a completely filled $4f$ shell, and thus there is no contribution from $4f$ electrons to the EFG. The observed EFG results entirely from the lattice charges and is expected to be almost constant with temperature. A measurement of the temperature dependence of the EFG is therefore a means to obtain information on the Yb ion charge state. An example is given in the next

section. Further examples can be found in Refs. [5, 6].

5. Yb charge states in Yb_3S_4

The Yb sulfide, Yb_3S_4, is known to be a heterogeneous mixed-valence system containing Yb^{3+} and Yb^{2+} ions. Such a conclusion was drawn already from crystallographic measurements [7]. In the crystal structure of Yb_3S_4, the ytterbium ions occupy three inequivalent sites. The analysis of distances between Yb sites and the nearest sulfur atoms allows in this case to distinguish divalent from trivalent ions. Recently this compound has aroused renewed interest because of the observation of Kondo-like low temperature specific heat properties [8], whereas its optical properties [9] and resistivity [10] are as those of a semiconductor with a gap of 0.4 eV.

Radioactive ^{172}Lu was produced directly in the sample of Yb_3S_4 during 20 MeV proton beam irradiation. The source was sealed in a quartz tube in vacuum and annealed at 700 K to remove irradiation defects. The PAC measurements were performed in the temperature range from 20 to 700 K using a standard, slow-fast coincidence setup with four detectors.

All Yb sites in Yb_3S_4 have a point symmetry lower than axial, thus the electric field gradient tensor at each site has to be described by two parameters, V_{zz} and η. According to crystal structure all PAC spectra were fitted assuming that the perturbation factor $R(t)$ is a sum of three components with equal weights. The thermal variations of the quadrupole interaction constant (proportional to V_{zz}) for the three components are shown in Fig. 4. For the component labelled with open symbols, V_{zz} is almost temperature independent, which corresponds to diamagnetic Yb^{2+} ions. For the two remaining components, labelled with solid

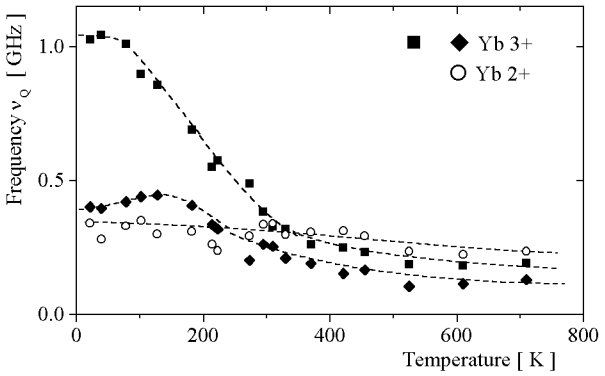

Fig. 4. EFG for three sites of Yb in Yb_3S_4. The dashed lines are to guide the eyes.

symbols, V_{zz} varies with temperature, which points to a Yb^{3+} charge state in the two lattice sites. A maximum observed around 150 K for one curve is attributed to a hybridization in one Yb^{3+} sublattice (see the last section for further explanation).

The mixed valence of Yb ions in Yb_3S_4 is also visible from the Mössbauer spectra taken in the antiferromagnetically ordered phase [11]. Below $T_N = 1.2$ K, a five-line magnetic hyperfine component develops, coexisting with the quadrupole broadened single line. The relative percentage of the magnetic component is 65(2)%, showing that two out of three Yb nuclei per formula unit experience a hyperfine field, so two out of three Yb ions are trivalent.

6. CEF influence on EFG

In some cases the temperature dependence of EFG for Yb^{3+} ions can be described quantitatively. The crystal electric field unambiguously determines the $V_{zz}(T)$ function. The CEF Hamiltonian can be written in equivalent operator formalism [12] as

$$\widehat{H}_{\mathrm{CEF}} = \sum_{n,m} B_n^m \widehat{O}_n^m, \tag{4}$$

where $\widehat{O}_n^m$ are the Stevens operators expressed by orbital momentum operators $\hat{J}_z$, $\hat{J}_\pm$, $\hat{J}^2$, and B_n^m are numerical coefficients. The number of nonzero coefficients in the sum depends on the point symmetry of the $4f$ ion in the crystal lattice. The EFG produced by the shell in a state $|\nu\rangle$ can be calculated as

$$\langle\nu|V_{ij}^{4f}|\nu\rangle = \beta^{4f}\langle\nu|\frac{3}{2}(\hat{J}_i\hat{J}_j + \hat{J}_j\hat{J}_i) - \delta_{ij}\hat{J}^2|\nu\rangle, \tag{5}$$

where the proportionality factor between the quadrupole moment of the $4f$ shell and the EFG produced by the shell for Yb^{3+} [13, 14] is equal to

$$\beta^{4f} = -30.5(1.5) \quad \mathrm{V/\AA^2}. \tag{6}$$

The average electric field gradient at temperature T is the Boltzmann average of all $4f$ levels

$$V_{ij}^{4f}(T) = \sum_\nu \langle\nu|V_{ij}^{4f}|\nu\rangle \exp(-E_\nu/kT) / \sum_\nu \exp(-E_\nu/kT), \tag{7}$$

where E_ν and $|\nu\rangle$ denote eigenvalues and eigenvectors of the $\widehat{H}_{\mathrm{CEF}}$ Hamiltonian. The lattice gradient can be linked with B_n^m parameters as well. When B_2^{-2} and B_2^2 coefficients vanish, and B_n^m's are expressed in kelvins, a simple relation is expected [14]

$$\beta^{\mathrm{lat}} = V_{zz}^{\mathrm{lat}}/B_2^0 = -10(4)\ \mathrm{V/(\AA^2\ K)} \quad (\text{for } Yb^{3+}). \tag{8}$$

The big uncertainty of β^{lat} is connected with the Sterncheimer antishielding factors $(1-\gamma_\infty)/(1-\sigma_2)$ which depend on the state of $4f$ shell and can be precisely calculated only for diamagnetic Yb^{2+} ions. The PAC measurements in $YbPO_4$ will illustrate how the above theory works in practice.

7. Crystal electric field in $YbPO_4$

The PAC measurements were performed in the temperature range 78–1000 K. Examples of spectra for the 91–1094 keV and 1094–79 keV cascades are shown in Fig. 5. The $YbPO_4$ crystallizes in a tetragonal lattice with a zircon structure. All

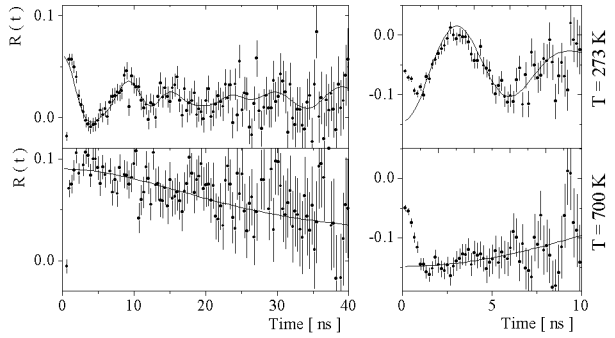

Fig. 5. PAC spectra measured in $YbPO_4$ using two $\gamma-\gamma$ cascades: left panels — 91–1094 keV, right panels — 1094–79 keV. Solid lines are fits with theoretical $G_{22}(t)$ for quadrupole interaction.

rare-earth ions in the crystal occupy equivalent positions of D_{2d} point symmetry, so the electric field gradient is axially symmetric and η is expected to be equal to zero. All spectra can be satisfactorily fitted assuming that all Yb nuclei are exposed to the same, axially symmetric electric field gradient. The temperature dependence of V_{zz} is shown in Fig. 6. The sign of V_{zz} was determined from the MS

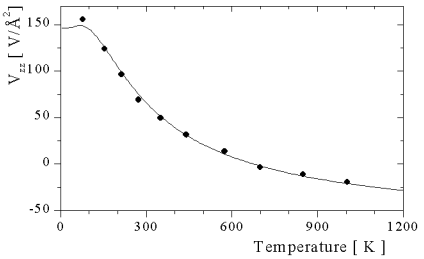

Fig. 6. Temperature dependence of EFG in $YbPO_4$. The solid line is the dependence calculated from known CEF coefficients (see text).

measurements at 4.2 K [15]. In the D_{2d} symmetry five independent B_n^m parameters describe the CEF interaction and

$$\widehat{H}_{\mathrm{CEF}} = B_2^0\widehat{O}_2^0 + B_4^0\widehat{O}_4^0 + B_4^4\widehat{O}_4^4 + B_6^0\widehat{O}_6^0 + B_6^4\widehat{O}_6^4. \tag{9}$$

Moreover, these parameters are known for $YbPO_4$ from inelastic neutron scattering measurements [16, 17] and

$$B_2^0 = 7.6,\ B_4^0 = 0.053,\ B_4^4 = 1.67,\ B_6^0 = -0.0082,\ B_6^4 = 0.02662 \text{ K}. \quad (10)$$

The excited $4f$ levels are located 140, 370, and 500 K above the ground state. The solid line in Fig. 6 is calculated on the basis of the above B_n^m coefficients. Only the two proportionality factors were fitted and the obtained values

$$\beta^{4f} = -33.9(6) \text{ V/Å}^2 \quad \text{and} \quad \beta^{\text{lat}} = -9.4(5) \text{ V/(Å}^2 \text{ K)} \quad (11)$$

are very close to theoretical predictions (6) and (8) and they are more precise.

8. Hybridization influence on EFG

In some intermetallic compounds of Yb, the hybridization between $4f$ and conduction electrons leads to anomalies in the specific heat and susceptibility [18]. While the magnetic Yb^{3+} ion has a nonzero spin $J = 7/2$, the screening conduction electrons can create a non-magnetic ground state in which the system does not order even at very low temperature. The magnetic susceptibility which is expected to be independent of temperature at low temperatures, is often enhanced compared to the ordinary Pauli paramagnetism of metals. A large electronic heat capacity yields a large Sommerfeld coefficient.

The hybridization in the moderate heavy fermion compounds can renormalize the CEF interaction, so it influences the electric field gradient. The interaction broadens the Kramers doublets, which gradually overlap each other. Since the sum of quadrupole moments of all CEF levels is equal to zero, the hybridizations leads to reduction of the $4f$ contribution to the EFG. A non-monotonic thermal variation of $V^{4f}(T)$ is expected even if the pure CEF interaction gives a strictly monotonically decreasing curve. Such a behavior was already observed in $YbCu_2Si_2$ [13] and $YbPd_2Si_2$ [19] compounds using the Mössbauer absorption with ^{174}Yb and ^{170}Yb probes and described theoretically by Zevin et al. [20].

9. Hybridization in $Yb_2Co_3Ga_9$

The $4f$ electronic state of Yb ion in $Yb_2Co_3Ga_9$ is strongly hybridized with the conduction electron band states, with a valency close to 2.9 as determined by L_{III}-edge X-ray absorption measurements. The Sommerfeld coefficient $\gamma = 116$ mJ/(mol K^2), which means that we have a moderate heavy fermion system [21]. The thermal variation of the $4f$ heat capacity, Pauli paramagnetic ground state, and thermal variation of susceptibility with a maximum around 50 K are well explained in the single-ion Coqblin–Schrieffer limit [22, 23] of the impurity spin $J = 7/2$, with a characteristic Kondo scale $T_0 = 260$ K [21].

The PAC measurements in $Yb_2Co_3Ga_9$ were performed in the range from 20 to 1000 K. $Yb_2Co_3Ga_9$ has orthorhombic crystal structure of $Y_2Co_3Al_9$-type with

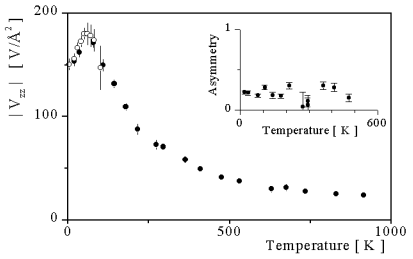

Fig. 7. Temperature dependence of EFG in $Yb_2Co_3Ga_9$ measured by ^{172}Yb PAC (solid points) and ^{170}Yb MS (open points).

a unique Yb site of low symmetry. The asymmetry parameter is measurable below 500 K and is found to be almost constant $\eta \approx 0.2$. The thermal variation of V_{zz} is shown in Fig. 7 by solid points. Open points in the figure originate from the Mössbauer absorption measurements in the temperature range from 4.2 to 100 K [24]. Both methods give the same values of V_{zz} in overlapping regions of temperature. A clearly visible maximum which is observed in the $V_{zz}(T)$ dependence around 50 K is the effect of hybridization.

10. Conclusions

The application of ^{172}Yb in the technique of perturbed angular correlation offers possibility to study hyperfine interactions of Yb-based compounds. Basic characteristics of this isotope as PAC probe were given. Various phenomena can be observed by measuring electric field gradients in Yb-based compounds. In Yb_3S_4 it was possible to differentiate between Yb^{2+} and Yb^{3+} ions which create a heterogeneous mixed-valence system. The crystal electric field influence on the EFG was quantitatively described in $YbPO_4$. Finally, an example of the reduction of the $4f$ quadrupole moment by the hybridization in $Yb_2Co_3Ga_9$ was presented.

References

[1] R.K. Rasera, A. Li-Scholz, *Phys. Rev. B* **1,** 1995 (1970).

[2] H. Frauenfelder, R.M. Steffen, in: *Alpha- Beta- Gamma-Ray Spectroscopy*, Ed. K. Siegbahn, North-Holland, Amsterdam 1968, Ch. XIXA.

[3] A.R. Arends, C. Hohenemser, F. Pleiter, H. de Ward, L. Chow, R.M. Suter, *Hyperfine Interact.* **8,** 191 (1980).

[4] P. Bonville, J.A. Hodges, Z. Hossain, R. Nagarajan, S.K. Dhar, L.C. Gupta, E. Alleno, C. Godart, *Eur. Phys. J. B* **11,** 377 (1999).

[5] M. Rams, K. Królas, K. Tomala, A. Ochiai, T. Suzuki, *Hyperfine Interact.* **97/98,** 125 (1996).

[6] M. Rams, K. Królas, P. Bonville, E. Alleno, C. Godart, D. Kaczorowski, F. Canepa, *Phys. Rev. B* **56,** 3690 (1997).

[7] P. Chevalier, P. Laruelle, J. Flahaut, Bull. Soc. Fr. Mineral. Crystallogr. **XC,** 564 (1967).

[8] Y.S. Kwon, Y. Haga, C. Ayache, T. Suzuki, T. Kasuya, *Physica B* **186,** 605 (1993).

[9] S. Kimura, Y.S. Kwon, T. Suzuki, T. Kasuya, *Physica B* **230,** 301 (1997).

[10] M.H. Jung, T.S. Park, H.J. Lee, Y.S. Kwon, *J. Korean Phys. Soc.* **32,** 71 (1998).

[11] M. Rams, K. Królas, P. Bonville, Y.S. Kwon, F. Gonzalez-Jimenez, *Physica B* **259,** 271 (1999).

[12] M.T. Hutchings, *Solid State Phys.* **16,** 227 (1964).

[13] K. Tomala, D. Weschenfelder, G. Czjzek, E. Holland-Moritz, *J. Magn. Magn. Mater.* **89,** 143 (1990).

[14] M. Rams, Ph.D. thesis, Jagiellonian University, Kraków 2000.

[15] J.A. Hodges, *J. Phys. (France)* **44,** 833 (1983).

[16] J. Nipko, M. Grimsditch, C.-K. Loong, S. Kern, M.M. Abraham, L.A. Boatner, *Phys. Rev. B* **53,** 2286 (1996).

[17] C.-K. Loong, M. Loewenhaupt, J.C. Nipko, M. Braden, L.A. Boatner, *Phys. Rev. B* **60,** 12549 (1999).

[18] E. Bauer, *Adv. Phys.* **40,** 417 (1991).

[19] P. Bonville, J. Hammann, J.A. Hodges, P. Imbert, G. Jehano, M.J. Besnus, A. Meyer, *Z. Phys. B* **82,** 267 (1991).

[20] V. Zevin, G. Zwicknagl, P. Fulde, *Phys. Rev. Lett.* **60,** 2331 (1998).

[21] S.K. Dhar, C. Mitra, P. Manfrinetti, A. Palenoza, P. Bonville, *Physica B* **259,** 150 (1990).

[22] V.T. Rajan, *Phys. Rev. Lett.* **51,** 308 (1983).

[23] C. Rossel, K.N. Yang, M.B. Maple, Z. Fisk, E. Zirngiebl, J.D. Thompson, *Phys. Rev. B* **35,** 1914 (1987).

[24] S.K. Dhar, C. Mitra, P. Bonville, M. Rams, K. Królas, C. Godart, E. Alleno, N. Suzuki, K. Miyake, N. Watanabe, Y. Onuki, P. Manfrinetti, A. Palenoza, *Phys. Rev. B* **64,** 094423 (2001).